Islamic Azad University

The Quarterly Journal of Optoelectronical Nanostructures

Summer 2016 / Vol. 1, No. 2

Dynamic Pull-in Instability of Nano-Actuators in the Presence of a Dielectric Layer

Mohammad Ghalambaz [*,1], Ali J. Chamkha [2], Mehdi Ghalambaz [1], Mohammad Edalatifar [3]

[1] Department of Mechanical Engineering, Dezful Branch, Islamic Azad University, Dezful, Iran.c Research Center.

[2] Mechanical Engineering Department, Prince Mohammad Bin Fahd University (PMU) P.O. Box 1664 Al-Khobar 31952, Kingdom of Saudi Arabia.

[3] Department of Electrical Engineering, Dezful Branch, Islamic Azad University, Dezful, Iran.

(Received 29 June 2016; Revised 14 July 2016; Accepted 15 Aug. 2016; Published 16 Sep 2016)

Abstract: The natural frequency and pull-in instability of clamped-clamped nano-actuators in the presence of a dielectric layer are analyzed. The influence of the presence of Casimir force, electrostatic force, fringing field effect, axial force, stretching effects and the size effect are taken into account. The governing equation of the dynamic response of the actuator is transformed in a non-dimensional form. The Galerkin decomposition method is employed to decompose the equations in time and space. Then, the obtained decomposed governing equations are solved numerically. The results show that the presence of the size effect and the axial force increases the natural frequency of the system. It is found that there is a unique value of the dielectric layer, in which the pull-in deflections of the nano-actuators are independent of the Casimir force, size effect and the axial loads. The advantage of this dielectric layer can be utilized in the design of nano-actuators and nano-sensors in the nanoscale.

Keywords: dielectric layer, nano-actuator, natural frequency, pull-in instability.

* Corresponding author. E-mail: m.ghalambaz@iaud.ac.ir

1. Introduction

A typical clamped-clamped nano-actuator is constructed using a moveable suspended conductive electrode over a substrate. Applying voltage difference between the electrode and the substrate induces an electro-static field, which attracts the moveable electrode into the substrate [1]. The system comprising of the electrode and the substrate can be seen as a capacitor, in which the capacity of the capacitor is a function of the deflection of the electrode. Hence, the deflection of the suspended electrode can be detected using electronic devices [2].

It is demonstrated that the nano-electro mechanical systems (NEMS) are good potential candidates to overcome many of the speed and sensitivity limitations of the conventional Micro-Electro-Mechanical Systems (MEMS) because of their very small size and tiny mass [3]. The NEMS devices and actuators have been utilized as nano-antennas and nano-switches [4], mass detection sensors [5, 6], hydrogen detection sensors [7], and nano-switches [8].

The experimental measurements show that when the structures are of the order of microns or sub-microns, the material properties exhibit the size-dependent effect in the torsion and bending tests of structures [9-11]. It is clear that the classical continuum theories are not capable of describing such size-dependent behaviors in small-scale elements. Thus, recently, several non-classical continuum theories, containing additional parameters for the material length scale, have been developed to capture the size effects [12].

Another issue, which is important in the nanoscale electro-mechanical systems, is the inter-molecular forces. As the size of a structure reduces to the dimension of a few nanometers, the inter-molecular forces become important, and they induce significant effects on the deflection and pull-in instability of the structures [13-15]. When the separation space between the electrode and the substrate is about 20 nm, retardation appears. In this case, the force between the nano-electrode and the substrate can be described by the Casimir force [16, 17]. In an ideal case, this force is proportional to the inverse fourth power of the separation [13, 18]. The Casimir force is usually negligible in micro-actuators, but is important in the design and operation of nano-actuators [14, 19]. The presence of an axial load [1, 20] is important in the fabrication and design of actuators. The axial loads are the results of the residual stress, because of the inconsistency of the properties of the nano-electrode. These axial loads are a crucial issue that should be accurately taken into account [21]. The presence of a dielectric layer can also significantly affect the behavior of a nano-actuator [16].

In a very recent study, Yazdanpanahi et al. [16] examined the static pull-in instability of nano-actuators in the presence of a layer of liquid dielectric over the substrate. They considered the effect of Casimir force on the behavior of the nano-actuator and found a unique value of the dielectric parameter, in which the

pull-in deflection of the nano-actuator is independent of the Casimir force. The presence of this unique dielectric layer reduces the nonlinearity of the nano-actuators and facilities design and application of these nano-electro-mechanical systems as sensors or other potential nano-scale devices. In the study of Yazdanpanahi et al. [16], the size effects and the axial loads were neglected. However, the literature review indicates that these effects are very important in the application and behavior of nano-actuators. In addition, to the best of authors' knowledge, the effect of the presence of a dielectric layer on the natural frequency and the dynamic behavior of the actuator has not yet been addressed.

The present study aims to analyze the dynamic pull-in instability and natural frequency of nano-actuators in the presence of a dielectric layer, Casimir effects, electrostatic forces, axial loads and considering the size effects. The presence of a unique dielectric layer, in which the pull-in deflections of the nano-actuators are independent of the axial loads, the Casimir forces and the size effects, is examined.

2. Mathematical model

A. The modified couple stress theory

The small-size effects are taken into account using the modified couple stress theory proposed by Yang et al. [22]. Based on the modified couple stress theory, the strain energy Ub in an isotropic linear elastic material is evaluated as [23]:

$$U_b = -\frac{1}{2}\int_0^l \left(M_X + N_{XY}\right)\frac{\partial^2 Y}{\partial X^2}dX \tag{1}$$

Where Y(x) is the displacement of the nanoelectrode; NXY and MX represent the couple moment and the resultant moment, respectively. For a beam type nanoelectrode NXY and MX are introduced as:

$$N_{XY} = \int_A \zeta_{XY} dA \tag{2}$$

$$M_X = \int_A \sigma_{XX} Z dA \tag{3}$$

Where A is the cross section area of the nanoelectrode. The ζ XY and σXX are defined as:

$$\zeta_{XY} = -\mu l_c^2 \frac{\partial^2 Y}{\partial X^2} \tag{4}$$

$$\sigma_{XX} = -EZ\frac{\partial^2 Y}{\partial X^2} \tag{5}$$

Where lc is the material length scale parameter of the nanoelectrode. E denotes the Young's modulus, and μ denotes the second Lame's constant (or the shear

modulus). Therefore, using Eqs. (4) and (5), the couple moment and the resultant moment, i.e. Eqs (2) and (3), are evaluated as:

$$N_{XY} = -\mu bhl^2 \frac{\partial^2 Y}{\partial X^2} \tag{6}$$

$$M_X = -E'I \frac{\partial^2 Y}{\partial X^2} \tag{7}$$

Where I denotes the moment of inertia of the nanoelectrode cross section, and E′ is the effective Young's modulus material of the nanoelectrode. The effective Young's modulus is (E′=E) for narrow beams (b<5h), and it becomes the plate modulus (E′=E/(1-υ2)) for wide beams (b>5h) where υ is the Poisson ratio.

B. Modeling of the nano-actuator

Consider a conductive nanoelectrode with a length l and a rectangular cross section A, which is suspended over a substrate. This type of actuators was fabricated by Hayamizu et al. [24] and analyzed in the work of Yazdanpanahi et al. [16]. The width of the nano-actuator is b, and its thickness is h. There is a layer of a dielectric over the substrate with a thickness hD and a permeability εD. The initial separation space between the nanoelectrode and the dielectric is g0. There is an external voltage difference V between the electrode and substrate, in which the voltage of the substrate is –V/2 and the voltage of the electrode is +V/2. The schematic view of the nano-actuator, geometric details and the coordinate system are shown in Fig. 1.

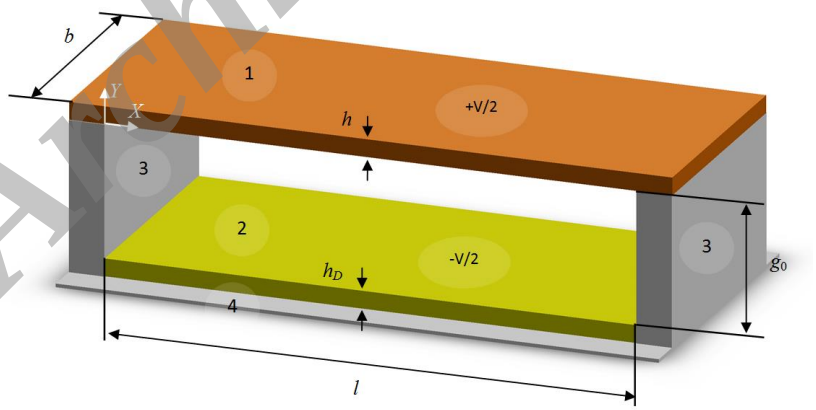

1-The moveable electrode, 2-Dielectric layer, 3-The fixed support, 4-The fixed conductive substrate.

Fig. 1: The schematic view of the clamped-clamped nano-actuator

The strain energy of the nano-actuator is evaluated by substituting the relations of the couple moment (Eq. (6)) and the resultant moment (Eq. (7)) into the strain energy equation (Eq. (1)) as:

$$U_b = \frac{1}{2}\int_0^l \left(E'I + \mu bhl_c^2\right)\left(\frac{\partial^2 Y}{\partial X^2}\right)^2 dX \tag{8}$$

The work done by a transverse external force, FEx, per unit length of the nanoelectrode is evaluated as [25]:

$$W_{Ex} = \int_0^l Y(X) F_{Ex} dX \tag{9}$$

The work due to the stretching and residual forces, Ua, in the nanoelectrode is evaluated as:

$$U_a = \frac{1}{2}\int_0^l \left(\hat{N} + T_a\right)\left(\frac{\partial^2 Y}{\partial X^2}\right)^2 dX \tag{10}$$

Where $\hat{N}$ denotes the residual forces and Ta is the additional axial force due to the mid-plane stretching. The axial force because of the mid-plane stretching, Ta, can be evaluated as:

$$T_a = \frac{E'bh}{2l}\int_0^l \left(\frac{\partial Y}{\partial X}\right)^2 dX \tag{11}$$

The total energy of the system is Π=Ub-Us-Wex+Ke where Ke is the kinematic energy of the nanoelectrode. Using the principle of the energy method, δΠ=δUb-δUs-δWex+δKe, the governing equation of the deflection for the nano-actuator is obtained as:

$$\left(E'I + \mu bhl_c^2\right)\frac{\partial Y^4}{\partial X^4} + \rho bh\frac{\partial Y^2}{\partial t^2} - \left(\frac{E'I}{2L}\int_0^l \left(\frac{\partial Y}{\partial X}\right)^2 dX + \hat{N}\right)\frac{\partial Y^2}{\partial X^2} = F_{Ex} \tag{12}$$

Where FEx is the sum of the Casimir force (Fc), electrostatic force (Fe) and the fringing field effect (Fr). The Casimir force per unit length of the beam, fc, can be evaluated as [26]:

$$f_c = \frac{\pi^2 hcb}{240\left(g_0 - Y\right)^4} \tag{13}$$

where h=1.055×10-34 Js is the reduced Planck's constant, and c is the light speed in vacuum such as c= 2.998×108 m/s. It should be noticed that Eq. (13) is valid for nano-actuators with widths (b) that are sufficiently higher than the separation space (g0). This assumption is valid for most of nano-actuators since, in most cases, the width of the electrode is much larger than the separation space [13, 27].

The electro-static force is the results of an applied external voltage between the substrate and the nanoelectrode. The electro-static force is the sum of the electro-static field and the fringing field effects, fe+fr. The electro-static force per

length of the beam can be evaluated using Maxwell's equations. Considering the first-order fringing field effects, the electro-static force is evaluated as [16]:

$$f_e + f_r = \frac{\varepsilon_0 b V^2}{2} \frac{1}{\left(\frac{h_D}{\varepsilon_D} + g_0 - h_D - Y \right)^2} + \frac{\varepsilon_0 V^2}{2} \frac{0.65}{g_0 - Y} \tag{14}$$

Where ε_0 is the permeability of the vacuum (ε_0=8.854×10-12 c^2/Nm^2). ε_D is the permeability of the dielectric layer and h_D is the thickness of the dielectric layer. The boundary conditions for a clamped-clamped nanoelectrode are written as:

$$Y(0,t) = \frac{\partial Y(0,t)}{\partial X} = 0, Y(l,t) = \frac{\partial Y(l,t)}{\partial X} = 0 \tag{15}$$

By using the following non-dimensional parameters:

$$y = \frac{Y}{g_0}, x = \frac{X}{l}, \tau = t\sqrt{\frac{E'I}{\rho b h l^4}} \tag{16-a}$$

$$\alpha = 6\frac{g_0}{h^2}, \kappa = \frac{(1-\varepsilon)h_D}{\varepsilon_D g_0}, \gamma = 0.65\frac{g_0}{b} \tag{16-b}$$

$$\alpha_c = \frac{\pi^2 h c b l^4}{240 E' I g_0^5}, N = \frac{\hat{N} l^2}{E'I}, \delta = \frac{\mu b h l_c^2}{E'I} \tag{16-c}$$

The non-dimensional governing equation for the nano-actuator is obtained as:

$$(1+\delta)\frac{\partial^4 y(x,\tau)}{\partial x^4} + \frac{\partial^2 y(x,\tau)}{\partial \tau^2} - \left(\alpha \int_0^1 \left(\frac{\partial y(x,\tau)}{\partial x} \right)^2 dx + N \right) \frac{\partial^2 y(x,\tau)}{\partial x^2} = \frac{\alpha_c}{(1-y(x,\tau))^4} + \frac{\beta}{(\kappa + 1 - y(x,\tau))^2} + \frac{\gamma\beta}{1-y(x,\tau)} \tag{17}$$

The non-dimensional boundary conditions are also as follow:

$$y(0,\tau) = \frac{\partial y(0,\tau)}{\partial x} = 0, \qquad y(1,\tau) = \frac{\partial y(1,\tau)}{\partial x} = 0 \tag{18}$$

3. Solution Method

The Galerkin decomposition method is employed herein to approximate Eq. (17) by a reduced-order model composed of the first discrete modal equation. The robustness of this method for dynamic analysis of actuators has been demonstrated in the study of Batra et al. [28]. The process starts by separating the dependences of the deflection of the deformed nanoelectrode using y(x,

τ)=ξ(τ)ϕ(x) where ξ(τ) captures the temporal dependence of the beam deflection and ϕ(x) is the first Eigen mode of the clamped-clamped beam satisfying the boundary conditions. ϕ(x) can be expressed by a polynomial as [29, 30]:

$$\phi(x)=16x^2(1-x)^2$$

Substituting y(x, τ)=ξ(τ)ϕ(x) in Eq. (17) results in

$$(1+\delta)\phi^{iv}\xi+\ddot{\xi}\phi-N\xi\phi''-\alpha\phi''\xi^3\int_0^1\phi'^2dx=f_{Ex}(\xi,\phi) \tag{19}$$

Where

$$f_{Ex}(\phi)=\frac{\alpha_c}{(1-\phi\xi)^4}+\frac{\beta}{(\kappa+1-\phi\xi)^2}+\frac{\gamma\beta}{1-\phi\xi} \tag{20}$$

Applying the Bubnov–Galerkin method gets

$$\ddot{\xi}\int_0^1\phi^2(x)dx+\left((1+\delta)\int_0^1\phi(x)\phi^{iv}(x)dx-N\int_0^1\phi(x)\phi''(x)dx\right)\xi -\alpha\left(\int_0^1\phi''(x)\phi(x)dx\right)\left(\int_0^1\phi'^2dx\right)\xi^3=\int_0^1 f_{Ex}(\xi)\phi(x)dx \tag{21}$$

where

$$f_{Ex}(\xi)=\alpha_c\int_0^1\frac{\phi(x)}{(1-\phi(x)\xi(\tau))^4}dx+\beta\int_0^1\frac{\phi(x)}{(\kappa+1-\phi(x)\xi(\tau))^2}dx+\gamma\beta\int_0^1\frac{\phi(x)}{1-\phi(x)\xi(\tau)}dx \tag{22}$$

Eq. (21) is rewritten in a more convenient form as:

$$a_2\ddot{\xi}+e_1\xi+e_2\xi^3=\alpha_c f_1(\xi)+\beta f_2(\xi)+\beta\gamma f_3(\xi) \tag{23}$$

where

$$e_1=\left((1+\delta)\int_0^1\phi(x)\phi^{iv}(x)dx-N\int_0^1\phi(x)\phi''(x)dx\right),$$

$$e_2=\alpha\left(\int_0^1\phi''(x)\phi(x)dx\right)\left(\int_0^1\phi'^2dx\right) \tag{24}$$

and

$$f_1(\xi)=\int_0^1\frac{\phi(x)}{(1-\phi(x)\xi(\tau))^4}dx \tag{25a}$$

$$f_2(\xi)=\int_0^1\frac{\phi(x)}{(\kappa+1-\phi(x)\xi(\tau))^2}dx \tag{25b}$$

$$f_3(\xi)=\int_0^1\frac{\phi(x)}{1-\phi(x)\xi(\tau)}dx \tag{25c}$$

Following the work of Batra et al. [28], the pull-in parameters are determined by discarding the inertia term in Eq. (23), i.e. $\ddot{\xi}$, and by requiring that the pull-in deflection should satisfy the resulting equation as:

$$e_1\xi_{PI} + e_2\xi_{PI}^3 = \alpha_c f_1(\xi_{PI}) + \beta f_2(\xi_{PI}) + \beta\gamma f_3(\xi_{PI}) \tag{26}$$

The pull-in deflection should also satisfy the nonlinear equation arising from differentiating both sides of Eq. (26) with respect to ξ [28, 31] as:

$$e_1 + 3e_2\xi_{PI}^2 = \alpha_c \dot{f}_1(\xi_{PI}) + \beta \dot{f}_2(\xi_{PI}) + \beta\gamma \dot{f}_3(\xi_{PI}) \tag{27}$$

Where

$$\dot{f}_1(\xi_{PI}) = 4\int_0^1 \frac{\phi^2(x)}{\left(1-\phi(x)\xi(\tau)\right)^5}dx \tag{28a}$$

$$\dot{f}_2(\xi_{PI}) = 2\int_0^1 \frac{\phi^2(x)}{\left(1-\phi(x)\xi(\tau)\right)^3}dx \tag{28b}$$

$$\dot{f}_3(\xi_{PI}) = \int_0^1 \frac{\phi^2(x)}{\left(1-\phi(x)\xi(\tau)\right)^2}dx \tag{28c}$$

Eqs. (26) and (27) can be solved simultaneously for any given set of prescribed non-dimensional parameters and an unknown non-dimensional parameter to obtain the corresponding value of ξPI. Then using the deduced ξPI, the pull-in value of the unknown parameter can be achieved. For example, assume a given set of the non-dimensional parameters of δ, η, αc, γ and κ and an unknown non-dimensional parameter of β. Solving Eqs. (26) and (27) for ξPI results in:

$$\begin{aligned} &e_1\left(\dot{f}_2(\xi_{PI}) + \gamma\dot{f}_3(\xi_{PI})\right)\xi_{PI} + e_2\left(\dot{f}_2(\xi_{PI}) + \gamma\dot{f}_3(\xi_{PI})\right)\xi_{PI}^3 \\ &\qquad - \alpha_c\left(\dot{f}_2(\xi_{PI}) + \gamma\dot{f}_3(\xi_{PI})\right)f_1(\xi_{PI}) \\ &\qquad = \beta\left(f_2(\xi_{PI}) + \gamma f_3(\xi_{PI})\right)\left(\dot{f}_2(\xi_{PI}) + \gamma\dot{f}_3(\xi_{PI})\right) \end{aligned} \tag{29}$$

and

$$\begin{aligned} &e_1\left(f_2(\xi_{PI}) + \gamma f_3(\xi_{PI})\right) + 3e_2\xi_{PI}^2\left(f_2(\xi_{PI}) + \gamma f_3(\xi_{PI})\right) \\ &\qquad - \alpha_c\dot{f}_1(\xi_{PI})\left(f_2(\xi_{PI}) + \gamma f_3(\xi_{PI})\right) = \\ &\qquad \beta\left(\dot{f}_2(\xi_{PI}) + \gamma\dot{f}_3(\xi_{PI})\right)\left(f_2(\xi_{PI}) + \gamma f_3(\xi_{PI})\right) \end{aligned} \tag{30}$$

Subtracting Eq. (30) from Eq. (29),

$$e_1\left(\left(\dot{f}_2(\xi_{PI})+\gamma\dot{f}_3(\xi_{PI})\right)\xi_{PI}-\left(f_2(\xi_{PI})+\gamma f_3(\xi_{PI})\right)\right)$$
$$+e_2\left(\left(\dot{f}_2(\xi_{PI})+\gamma\dot{f}_3(\xi_{PI})\right)\xi_{PI}^3-3\xi_{PI}^2\left(f_2(\xi_{PI})+\gamma f_3(\xi_{PI})\right)\right) \quad (31)$$
$$-\alpha_c\left(\left(\dot{f}_2(\xi_{PI})+\gamma\dot{f}_3(\xi_{PI})\right)f_1(\xi_{PI})-\dot{f}_1(\xi_{PI})\left(f_2(\xi_{PI})+\gamma f_3(\xi_{PI})\right)\right)=0$$

It is worth noticing that the functions f and $\dot{f}$ were defined in Eqs. (25) and (28), respectively. As seen, the functions f and $\dot{f}$ are in an integral form as a function of ξ. Thus, Eq. (31) should be solved numerically for the pull-in value of ξPI. Later, the deduced value of ξPI can be substituted into Eq. (29) to evaluate the pull-in electro-static parameter (βPI) as:

$$\beta_{PI}=\frac{e_1\xi+e_2\xi^3-\alpha_c f_1(\xi)}{f_2(\xi)+\gamma f_3(\xi)} \quad (32)$$

In order to evaluate the oscillation frequency of the nano-actuator after deflection, Eq (26) should be solved for the basic deflection of the beam ($\bar{\xi}$). Then, assuming $\xi=\bar{\xi}+\Delta\xi$, the governing equation (23) is rewritten as [28, 31]:

$$a_2\Delta\ddot{\xi}+e_1\left(\bar{\xi}+\Delta\xi\right)+e_2\left(\bar{\xi}+\Delta\xi\right)^3= \alpha_c f_1\left(\bar{\xi}+\Delta\xi\right)+\beta f_2\left(\bar{\xi}+\Delta\xi\right)+\beta\gamma f_3\left(\bar{\xi}+\Delta\xi\right) \quad (33)$$

where retaining only the linear terms in $\Delta\xi$ gives:

$$a_2\Delta\ddot{\xi}+e_1\bar{\xi}+e_1\Delta\xi+e_2\bar{\xi}+3e_2\bar{\xi}^2\Delta\xi= \alpha_c f_1\left(\bar{\xi}\right)+\alpha_c\Delta\xi\dot{f}_1\left(\bar{\xi}\right)+\beta f_2\left(\bar{\xi}\right)+\beta\Delta\xi\dot{f}_2\left(\bar{\xi}\right)+\beta\gamma f_3\left(\bar{\xi}\right)+\beta\gamma\Delta\xi\dot{f}_3\left(\bar{\xi}\right) \quad (34)$$

Since $\bar{\xi}$ is the solution of Eq. (27), the above equation is simplified as:

$$a_2\Delta\ddot{\xi}+e_1\Delta\xi+3e_2\bar{\xi}^2\Delta\xi=\alpha_c\Delta\xi\,\dot{f}_1\left(\bar{\xi}\right)+\beta\Delta\xi\,\dot{f}_2\left(\bar{\xi}\right)+\beta\gamma\Delta\xi\,\dot{f}_3\left(\bar{\xi}\right) \quad (35)$$

Now, a harmonic solution of $\Delta\xi=\Delta\xi_0 e^{i\omega\tau}$ is assumed where $i=\sqrt{-1}$ and ω is the oscillation frequency. Substituting $\Delta\xi=\Delta\xi_0 e^{i\omega\tau}$ into Eq. (35) yields:

$$-a_2\Delta\xi_0\omega^2 e^{i\omega\tau}+e_1\Delta\xi_0 e^{i\omega\tau}+3e_2\bar{\xi}^2\Delta\xi_0 e^{i\omega\tau}= \alpha_c\Delta\xi_0 e^{i\omega\tau}\dot{f}_1\left(\bar{\xi}\right)+\beta\Delta\xi_0 e^{i\omega\tau}\dot{f}_2\left(\bar{\xi}\right)+\beta\gamma\Delta\xi_0 e^{i\omega\tau}\dot{f}_3\left(\bar{\xi}\right) \quad (36)$$

Dividing both sides of Eq. (36) by $\Delta\xi_0 e^{i\omega\tau}$ gives:

$$-a_2\omega^2+e_1+3e_2\bar{\xi}^2=\alpha_c\,\dot{f}_1\left(\bar{\xi}\right)+\beta\,\dot{f}_2\left(\bar{\xi}\right)+\beta\gamma\,\dot{f}_3\left(\bar{\xi}\right) \quad (37)$$

and solving for the angular frequency of ω results:

$$\omega(\tau)=\sqrt{\frac{e_1+3e_2\bar{\xi}^2-\alpha_c\dot{f_1}(\bar{\xi})-\beta\dot{f_2}(\bar{\xi})-\beta\gamma\dot{f_3}(\bar{\xi})}{a_2}} \tag{38}$$

Therefore, the fundamental frequency of the nano-actuator can be obtained using Eq. (38) for any prescribed set of non-dimensional parameters. When the non-dimensional parameters of the nano-actuator tends to the pull-in parameters, the frequency of the nano-actuator, $\omega(\tau)$, suddenly drops and tends to zero. This effect is noticed in the work of [20] in the study of micro-beams. Therefore, it can be concluded that, at the onset of the pull-in instability, the fundamental frequency of the actuator is zero.

4. Validation

By neglecting the size effect, the dielectric layer and the Casimir forces (i.e. $\delta=0$, $\alpha c=0$, $\kappa=0$), the present study reduces to the analysis of a micro-actuator. In this case, Tilmans and Legtenberg [32] experimentally analyzed the vibration of micro-actuators with different lengths. The properties of the proposed micro-beams are shown in Table 1. A comparison between the results of the present study and the experimental results reported by Tilmans and Legtenberg [32] as well as the theoretical results reported by Abdel-Rahman et al. [20] is performed in Fig. 2. Fig. 2 shows the normalized natural frequency of the actuators ($\omega/\omega 0$) as a function of the electro-static parameter for two actuators with the lengths of 210 μm and 510 ηm; where $\omega 0$ is the fundamental frequency of the actuator without any applied voltage.

The pull-in voltage of the micro-actuators, proposed in Table 1, are evaluated using the present method and the results are compared with the experimental results reported by Tilmans and Legtenberg [32] as well as the analytical results reported by Kuang and Chen [33] in Table 2. The fundamental frequency is obtained from the solution of Eq. (38). The pull-in voltages are calculated from Eqs. (31) and (32). The integral terms, i.e. f and $\dot{f}$, are calculated numerically using the Gaussian quadrature integral method with the relative error of 10-12. The roots of the functions are calculated using the Newton method with the relative error of 10-12.

Yazdanpanahi et al. [16] examined the static deflection and pull-in instability of nano-actuators in the presence of a dielectric layer. Therefore, neglecting the axial load and size effects ($\delta=0$ and $N=0$), the evaluated maximum deflection of the nano-actuator is compared with the results reported by Yazdanpanahi et al. [16]. Considering, $\beta=5$, $\gamma=0.065$, $\alpha=0.96$, $\alpha c=20$ and $\kappa=-0.396$, the maximum static deflection of the actuator is evaluated as $\xi=0.1354$ in the study of Yazdanpanahi et al. [16]. In the present study and assuming ($\delta=0$ and $N=0$), the maximum deflection is obtained as $\xi=0.1341$, which shows good agreement with the static deflection of the nano-actuator reported by Yazdanpanahi et al. In this

case, the analysis of the dynamic response of the system shows that the non-dimensional natural frequency of the nano-actuator, ω(τ), is 18.5.

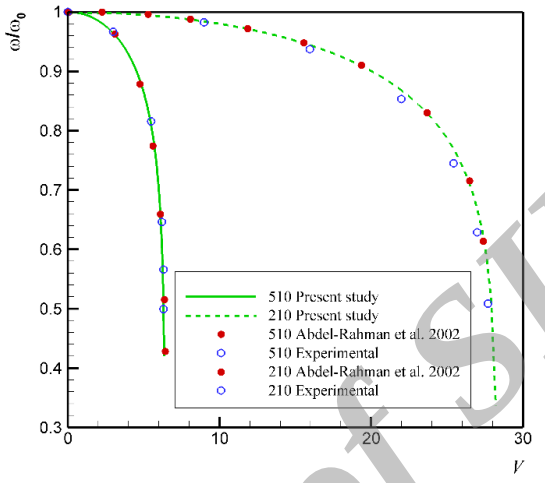

Fig. 2. A comparison between the natural frequencies of the actuators (proposed in Table 1) with lengths of 210μm and 510μm.

5. Results and Discussion

A. *free vibration*

In this section, the effect of the non-dimensional parameters on the deflection and the fundamental frequency of nano-actuators is analyzed. The results of this section are obtained from the numerical solution of Eqs. (27) and (38).

Figs. 3 and 4 show the influence of the dielectric parameter (κ) and the size effect parameter (δ) on the deflection and the natural frequency of the nano-actuator, respectively. The presence of the size effect, because of the nano-size of the actuator, tends to harden the actuator. Hence, as seen in Fig. 3, the presence of the size effect reduces the maximum deflection (u(τ)) of the nano-actuator. Fig. 3 shows that an increase in the magnitude of the dielectric parameter increases the maximum deflection of the nano-actuator. Indeed, the presence of the dielectric layer magnifies the strength of the electro-static force and results in higher deflections of the actuator. The effect of variation of the size effect parameter is more significant in the case of high magnitudes of the dielectric parameter. Fig. 4 shows that the presence of the dielectric layer decreases the natural frequency of the actuator. In contrast, the presence of the size effect increases the natural frequency of the nano-actuator. In the case of high magnitudes of the dielectric parameter, the natural frequency of the nano-actuator drops rapidly.

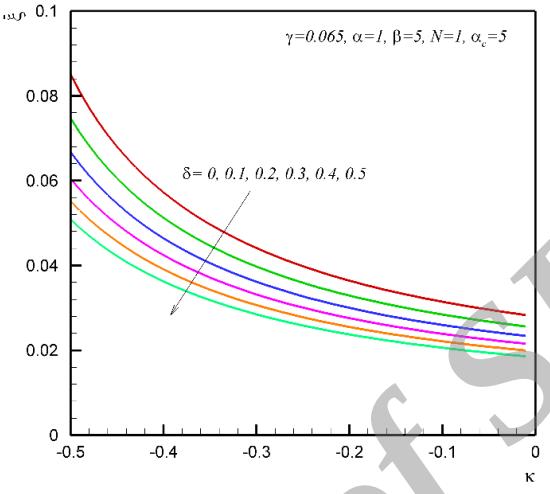

Fig. 3. The maximum deflection of the nano-actuator as a function of the dielectric parameter (κ) for selected values of the size effect parameter (δ).

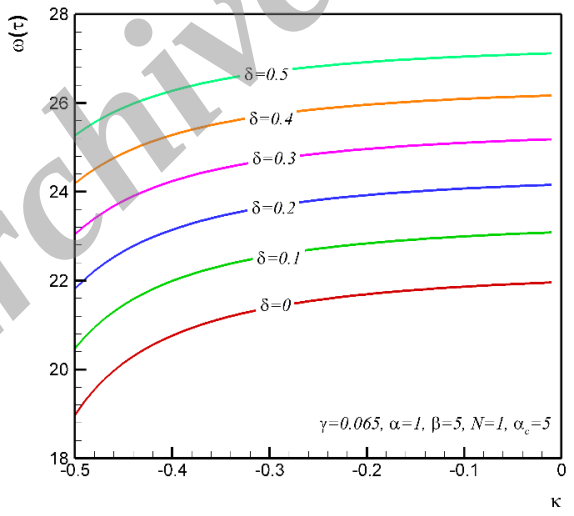

Fig. 4. The natural frequency of the nano-actuator as a function of dielectric parameter (κ) for selected values of the size effect parameter (δ).

Figs. 5 and 6 show the maximum deflection and the natural frequency of the nano-actuators, respectively, as a function of the dielectric layer parameter for selected values of the axial load parameter. These figures show that the presence of the axial load decreases the maximum deflection of the nano-actuator, but it increases the natural frequency of the actuator. The presence of the initial tensile in the actuator induces the hardening effects. The results of these figures which are in agreement with the results of Figs. 3 and 4 indicate that the increase of the magnitude of the dielectric parameter raises the maximum deflection of the nano-actuator and reduces its natural frequency. Abdel-Rahman et al. [20] studied the dynamic vibration of micro-actuators subject to electro-static forces and found that the electro-static force provides a softening effect on the overall mechanical stiffness, while the membrane stretching introduces strain hardening. The results of present study are in good agreement with the results of Abdel-Rahman et al. [20].

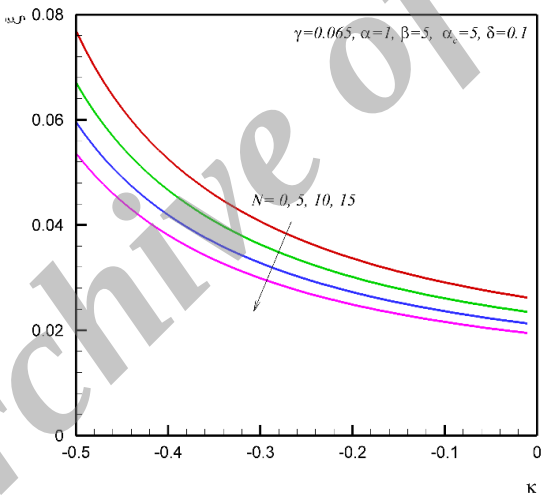

Fig. 5. Maximum deflection of the nano-actuator ($u(\tau)$) as a function of the dielectric parameter (κ) for selected values of the axial load parameter (N).

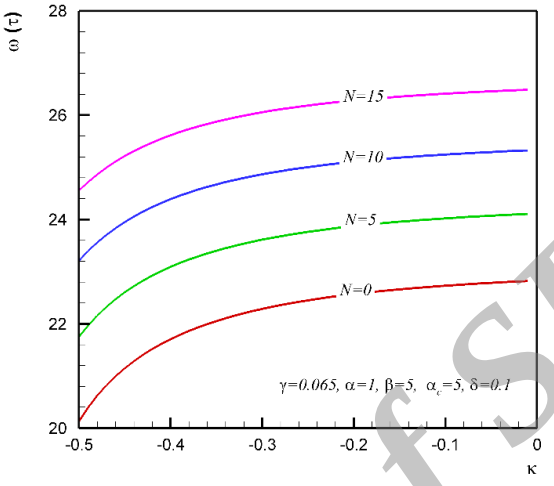

Fig. 6. Natural frequency of the nano-actuator ($\omega(\tau)$) as a function of the dielectric parameter (κ) for selected values of the axial load parameter (N).

B. Pull-in stability analysis

The results of this section are obtained from the numerical solution of Eqs. (31) and (32). The pull-in deflection and the pull-in electrostatic parameter as a function of the pull-in dielectric parameter are plotted in Figs. 7 and 8, respectively for selected values of the size effect parameter. Fig. 7 shows that as the magnitude of the dielectric parameter ($|\kappa|$) increases, the pull-in deflection decreases. This observation is in contrast with the trends of the results of Fig. 3. Indeed, the increase of the magnitude of the dielectric parameter magnifies the effect of the electro-static force and hence, increases the deflection of the nano-actuator. However, at the onset of the pull-in instability, the pull-in occurs with larger gap sizes because of the larger electro-static forces. In other word, when the presence of a dielectric layer magnifies the electro-static force, the applied force gets enough strength to induce the pull-in instability merely after a small deflection of the nano-actuator. Thus, the pull-in deflection in the presence of a dielectric layer is lower than that of the regular nano-actuators without a dielectric layer (i.e. $\kappa=0$).

Fig. 8 depicts that an increase in the magnitude of the dielectric parameter, significantly decreases the magnitude of the pull-in electrostatic parameter (β_{PI}). As the magnitude of the dielectric parameter increases, the influence of the size effect parameter on the variation of the pull-in electro-static parameter (β_{PI}) reduces. The variation of the size effect parameter in Fig. 7 reveals that there is a

focal point in which the magnitude of the deflection of the nano-actuator is independent of the size effect. As seen, the magnitude of this dielectric parameter is -0.39. Here, this special dielectric parameter is denoted by κ*.

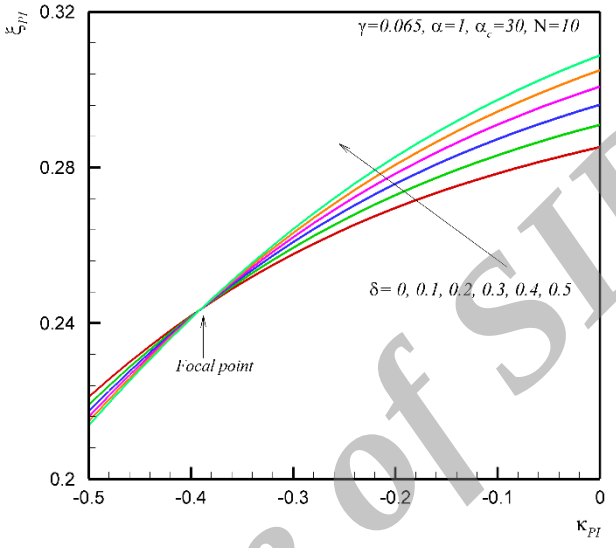

Fig. 7. The pull-in deflection of the nano-actuators as a function of the pull-in dielectric parameter for selected values of the size effect parameter.

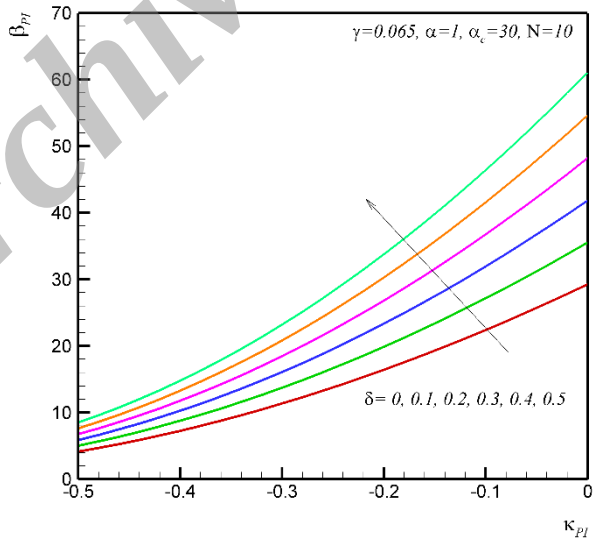

Fig. 8. The pull-in electrostatic parameter (β_{PI}) as a function of the pull-in dielectric parameter for selected values of the size effect parameter (δ).

Fig. 9 depicts the pull-in deflection of nano-actuators as a function of the dielectric parameter for selected values of the axial load parameter. Fig. 10 shows the corresponding pull-in voltages of Fig. 9. Fig. 9 shows that an increase in the magnitude of the dielectric parameter, decreases the pull-in deflection. The trend of the results of Fig. 9 are in full agreement with the trend of the results of Fig. 7 in the present study as well as Fig. 8 in the study of Yazdanpanahi et al. [16]. Fig. 10 shows that increasing the magnitude of the dielectric parameter, significantly reduces the pull-in electrostatic parameter. In contrast, increasing the axial load, increases the pull-in electrostatic parameter. However, the influence of the axial load parameter on the pull-in electro-static parameter reduces as the dielectric parameter gets stronger. Fig. 9 indicates a focal point for the axial load parameter (N). This focal point shows that there is a magnitude for the dielectric parameter in which the variation of the axial load does not affect the pull-in deflection of the nano-actuator. In this figure, the corresponding non-dimensional dielectric parameter (κ*) is -0.39.

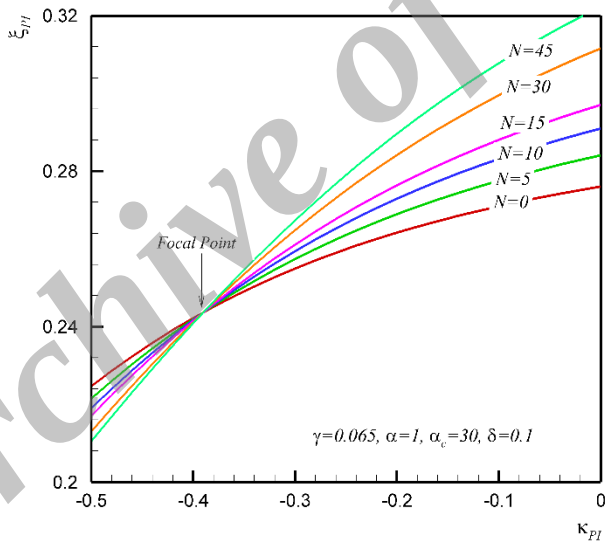

Fig. 9. The pull-in deflection of the nano-actuators as a function of the pull-in dielectric parameter for selected values of the axial load parameter (*N*).

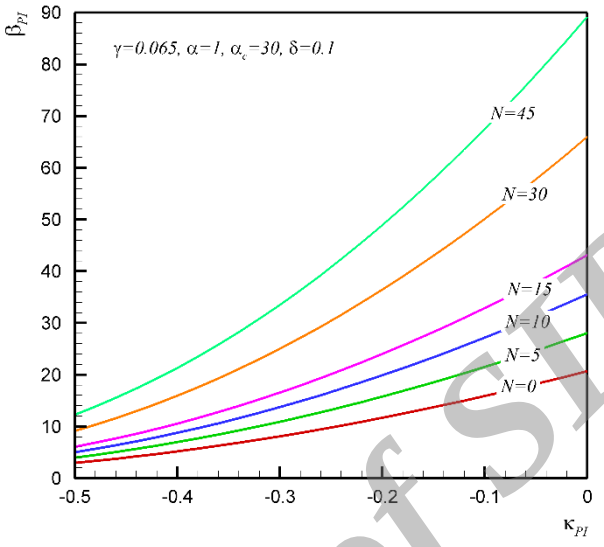

Fig. 10. The pull-in electrostatic parameter (β_{PI}) as a function of the pull-in dielectric parameter for selected values of the axial load parameter (N).

Fig. 11 presents the pull-in deflection of the nano-actuator as a function of the dielectric parameter for selected values of the Casimir parameter. Fig. 12 displays the corresponding pull-in electro-static parameters of Fig. 11. These figures are in agreement with Figs. 7-10 as they depict that an increase in the magnitude of the dielectric parameter, decreases the pull-in deflection (ξPI) as well as the electrostatic pull-in parameter (βPI). Fig. 12 shows that the presence of the Casimir effect reduces the pull-in values of the electrostatic parameter (βPI). Fig. 11 indicates that there is a focal point for the pull-in deflection of the nano-actuator, in which the variations of the Casimir parameter do not affect the pull-in deflection of the actuator. The corresponding dielectric parameter for this focal point (κ*) is - 0.395. This magnitude for the dielectric parameter is almost the same as that of Figs. 7 and 9. Therefore, designing a nano-actuator with a dielectric parameter of κ*≈-0.39 results in a nano-actuator, in which its pull-in instability deflection is not sensitive to the size effect, axial loads or the Casimir forces.

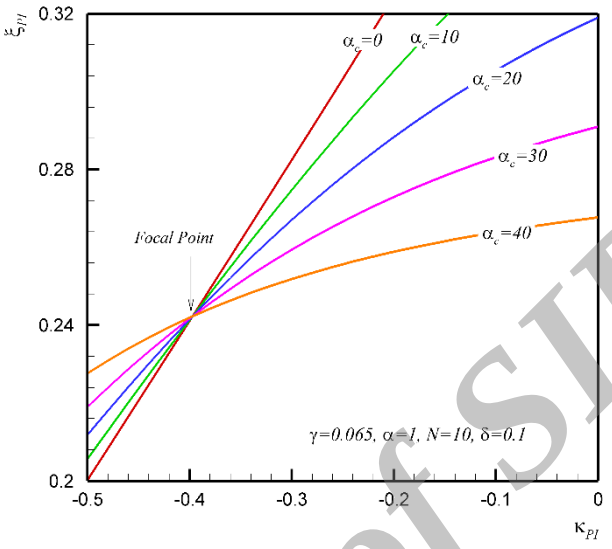

Fig. 11. The pull-in deflection of the nano-actuators as a function of pull-in dielectric parameter for selected values of the Casimir parameter (α_c).

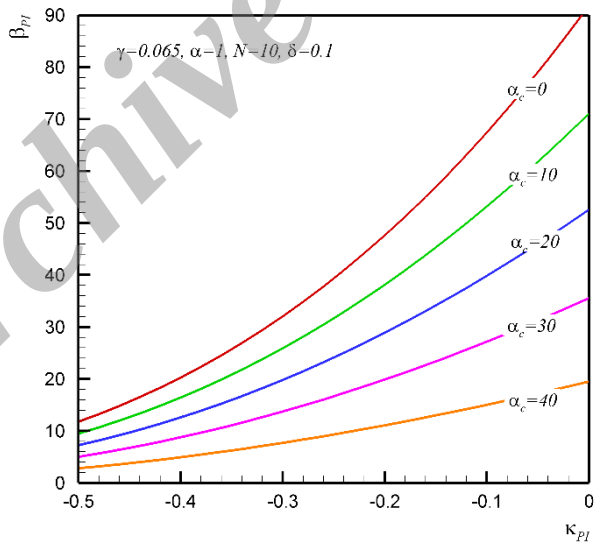

Fig. 12. The pull-in electrostatic parameter (β_{PI}) as a function of the pull-in dielectric parameter for selected values of the Casimir parameter (α_c).

Such a focal point, which eliminates the non-linear effects of the Casimir force, size effect and the axial loads, is crucial in the design of nano-actuator sensors. This observed focal point facilities the design of nano-actuators and nanosensors in nano-scale sizes.

6. Conclusion

The dynamic oscillation, deflection and pull-in instability of the clamped-clamped nano-actuators in the presence of a dielectric layer, Casimir force effect, size effect, electro-static forces and axial loads are analyzed. The results are compared with the experimental and theoretical results available in literature and are found in good agreement. The results of the present study can be summarized as follows:

1- The presence of the size effect and the axial loads decreases the deflection of the nano-actuator, but the presence of these effects increases the natural frequency of the system.

2- The presence of a dielectric layer significantly increases the deflection of the nano-actuator and decreases its natural frequency.

3- The presence of the size effect, axial loads and the dielectric layer raises the pull-in voltage of the system. In contrast, the presence of the Casimir force effect reduces the pull-in voltage.

4- There is a unique value for the dielectric layer parameter (κ^*) in which the pull-in deflections of the nano-actuators are independent of the variation of the size effect, the Casimir force effect and the axial forces.

5- The value of κ^* is obtained to be about -0.39 in the present study

As mentioned, the system of the nano-electrode and the substrate constructs a capacity. Indeed, a nano-actuator in the presence of an electro-static force is a nano-capacitor. The deflection of this nano-capacitor changes the capacity of the system, which later can be detected by electronic devices. Hence, the obtained value for the dielectric parameter in which the deflection of the nano-actuator is independent of the fabrication process (the initial tensile which leads to axial loads) and the nano-size effects (the Casimir force and the size effect) can be facilitated in the design of nano-actuators and nano-sensors. The future studies can be focused on the fabrication methods of these new types of nano-actuators and experimental validation of the evaluated value of the obtained dielectric parameter.

Acknowledgements

The authors are grateful to Dezful Branch, Islamic Azad University for its support.

7. References

[1] R. Soroush, A.L.I. Koochi, A.S. Kazemi, M. Abadyan, *Modeling the Effect of Van Der Waals Attraction on the Instability of Electrostatic Cantilever and Doubly-Supported Nano-Beams Using Modified Adomian Method*, International Journal of Structural Stability and Dynamics, 12 (2012) 1250036.

[2] R. Ansari, R. Gholami, M.F. Shojaei, V. Mohammadi, S. Sahmani, *Surface stress effect on the pull-in instability of circular nanoplates*, Acta Astronautica, 102 (2014) 140-150.

[3] M.A. Cullinan, R.M. Panas, C.M. DiBiasio, M.L. Culpepper, *Scaling electromechanical sensors down to the nanoscale*, Sensors and Actuators A: Physical, 187 (2012) 162-173.

[4] S. Demoustier, E. Minoux, M. Le Baillif, M. Charles, A. Ziaei, *Review of two microwave applications of carbon nanotubes: nano-antennas and nano-switches*, Comptes Rendus Physique, 9 (2008) 53-66.

[5] K. Kiani, Q. Wang, *On the interaction of a single-walled carbon nanotube with a moving nanoparticle using nonlocal Rayleigh, Timoshenko, and higher-order beam theories*, European Journal of Mechanics - A/Solids, 31 (2012) 179-202.

[6] H.S. Wasisto, S. Merzsch, A. Stranz, A. Waag, E. Uhde, T. Salthammer, E. Peiner, *Silicon resonant nanopillar sensors for airborne titanium dioxide engineered nanoparticle mass detection*, Sensors and Actuators B: Chemical, 189 (2013) 146-156.

[7] M.-O. Kim, K. Lee, H. Na, D.-S. Kwon, J. Choi, J.-I. Lee, D.-H. Baek, J. Kim, *Highly sensitive cantilever type chemo-mechanical hydrogen sensor based on contact resistance of self-adjusted carbon nanotube arrays*, Sensors and Actuators B: Chemical, 197 (2014) 414-421.

[8] M. Liao, Z. Rong, S. Hishita, M. Imura, S. Koizumi, Y. Koide, *Nanoelectromechanical switch fabricated from single crystal diamond: Experiments and modeling*, Diamond and Related Materials, 24 (2012) 69-73.

[9] L.-L. Ke, Y.-S. Wang, J. Yang, S. Kitipornchai, *Free vibration of size-dependent Mindlin microplates based on the modified couple stress theory*, Journal of Sound and Vibration, 331 (2012) 94-106.

[10] D.C.C. Lam, F. Yang, A.C.M. Chong, J. Wang, P. Tong, *Experiments and theory in strain gradient elasticity*, Journal of the Mechanics and Physics of Solids, 51 (2003) 1477–1508.

[11] A.W. McFarland, J.S. Colton, *Role of material microstructure in plate stiffness with relevance to microcantilever sensors*, Journal of Micromechanics and Microengineering, 15 (2005) 1060–1067.

[12] M. Mohammad-Abadi, A.R. Daneshmehr, *Size dependent buckling analysis of microbeams based on modified couple stress theory with high order theories and general boundary conditions*, International Journal of Engineering Science, 74 (2014) 1-14.

[13] A. Koochi, A.S. Kazemi, Y. Tadi Beni, A. Yekrangi, M. Abadyan, *Theoretical study of the effect of Casimir attraction on the pull-in behavior of beam-type NEMS using modified Adomian method*, Physica E: Low-dimensional Systems and Nanostructures, 43 (2010) 625-632.

[14] A. Farrokhabadi, N. Abadian, R. Rach, M. Abadyan, *Theoretical modeling of the Casimir force-induced instability in freestanding nanowires with circular cross-section*, Physica E: Low-dimensional Systems and Nanostructures, 63 (2014) 67-80.

[15] A. Farrokhabadi, R. Rach, M. Abadyan, *Modeling the static response and pull-in instability of CNT nanotweezers under the Coulomb and van der Waals attractions*, Physica E: Low-dimensional Systems and Nanostructures, 53 (2013) 137-145.

[16] E. Yazdanpanahi, A. Noghrehabadi, M. Ghalambaz, *Pull-in instability of electrostatic doubly clamped nano actuators: Introduction of a balanced liquid layer (BLL)*, International Journal of Non-Linear Mechanics, 58 (2014) 128-138.

[17] H. M. Sedighi, F. Daneshmand, J. Zare, *The influence of dispersion forces on the dynamic pull-in behavior of vibrating nano-cantilever based NEMS including fringing field effect*. Archives of Civil and Mechanical Engineering, (In Press). DOI: 10.1016/j.acme.2014.01.004.

[18] A. Gusso, G.J. Delben, *Dispersion force for materials relevant for micro and nanodevices fabrication*, Journal of Physics D, Applied Physics, 41 (2008) 175405.

[19] A. Koochi, A.S. Kazemi, A. Noghrehabadi, A. Yekrangi, M. Abadyan, *New approach to model the buckling and stable length of multi walled carbon nanotube probes near graphite sheets*, Materials & Design, 32 (2011) 2949-2955.

[20] E.M. Abdel-Rahman, M.I. Younis, A.H. Nayfeh, *Characterization of the mechanical behavior of an electrically actuated microbeam*, Journal of Micromechanics and Microengineering 12 (2002) 759–766.

[21] L.X. Zhang, Y.P. Zhao, *Electromechanical model of RF MEMS switches*, Microsyst. Technol., 9 (2003) 420-426.

[22] F. Yang, A.C.M. Chong, D.C.C. Lam, P. Tong, *Couple stress based strain gradient theory for elasticity*, Int. J. Solids Struct., 39 (2002) 2731–2743.

[23] S.K. Park, X.L. Gao, *Bernoulli–Euler beam model based on a modified couple stress theory*, J. Micromech. Microeng., 16 (2006) 2355–2359.

[24] Y. Hayamizu, T. Yamada, K. Mizuno, R.C. Davis, D.N. Futaba, M. Yumura, K. Hata, *Integrated three-dimensional microelectromechanical devices from processable carbon nanotube wafers*, Nature Nanotechnology, 3 (2008) 289–294.

[25] F.P. Beer, J.H. Johnston, J.T. Dewolf, D.F. Mazurek, *Mechanics of Material*, 5th ed., Mc-Graw Hill Companies, New York, 2009.

[26] A. Ramezani, A. Alasty, J. Akbari, *Pull-in parameters of cantilever type nanomechanical switches in presence of Casimir force*, Nonlinear Analysis: Hybrid Systems, 1 (2007) 364-382.

[27] A. Ramezani, A. Alasty, J. Akbari, *Closed-form solutions of the pull-in instability in nano-cantilevers under electrostatic and intermolecular surface forces*, International Journal of Solids and Structures, 44 (2007) 4925-4941.

[28] R.C. Batra, M. Porfiri, D. Spinello, *Vibrations of narrow microbeams predeformed by an electric field*, Journal of Sound and Vibration, 309 (2008) 600-612.

[29] R.C. Batra, M. Porfiri, D. Spinello, *Electromechanical model of electrically actuated narrow microbeams*, J Microelectromech Syst, 15 (2006) 1175–1189.

[30] M. Moghimi Zand, M.T. Ahmadian, *Application of homotopy analysis method in studying dynamic pull-in instability of microsystems*, Mechanics Research Communications, 36 (2009) 851-858.

[31] R.C. Batra, M. Porfiri, D. Spinello, *Vibrations and pull-in instabilities of microelectromechanical von Kármán elliptic plates incorporating the Casimir force*, Journal of Sound and Vibration, 315 (2008) 939-960.

[32] H.A. Tilmans, R. Legtenberg, *Electrostatically driven vacuum-encapsulated polysilicon resonators: Part II. Theory and performance*, Sensors Actuators A, 45 (1994) 67–84.

[33] J.H. Kuang, C.-J. Chen, *Dynamic characteristics of shaped micro-actuators solved using the differential quadrature method*, Journal of Micromechanics and Microengineering, 14 (2004) 647-655.